APEM journal
Advances in Production Engineering & Management **ISSN 1854-6250**
Volume 15 | Number 2 | June 2020 | pp 179–191 Journal home: apem-journal.org
https://doi.org/10.14743/apem2020.2.357 Original scientific paper

Fuel gas operation management practices for reheating furnace in iron and steel industry

Chen, D.M.[a,b]**, Liu, Y.H.**[a]**, He, S.F.**[c]**, Xu, S.**[c]**, Dai, F.Q.**[b]**, Lu, B.**[a,*]

[a]School of Civil Engineering and Architecture, Anhui University of Technology, Ma'anshan, P.R. China
[b]The State Key Laboratory of Refractories and Metallurgy, Wuhan University of Science and Technology, Wuhan, P.R. China
[c]Ma'anshan iron and Steel Co., Ltd, Ma'anshan, Anhui, P.R. China

ABSTRACT

How to evaluate the fuel gas operation (FGO) of various working groups (WGs) and working shifts (WSs) in reheating furnace is still ambiguous problem. In this paper, a novelty time-series FGO evaluation model was proposed. The strategy mainly included: Firstly, the fuel gas per ton steel (FGTS) was calculated in certain time interval; Secondly, the FGTS time-series data set was formulated in statistical period; Thirdly, the FGTS time-series data set was divided according to working schedule; Lastly, the FGO evaluation model was established. Case study showed that: i) The fuel gas operation evaluation results of various WGs in different WSs were accorded with normal distribution; ii) For various WGs, A WG performed best, followed by C WG and D WG. The performance of B WG was the worst due to its violent fluctuation of fuel gas operation evaluation results in three WSs; iii) For different WSs, the day WS and swing WS performed well, whereas the performance of night WS was unsatisfactory. Discussion results showed that the improvement of working skills, working responsibility and working passion, which were effective measure to achieve energy saving in terms of operation, should be enhanced through skills training and the reward and punishment system. Generally, this novelty time-series FGO evaluation method could also be applied to other industrial equipment.

ARTICLE INFO

Keywords:
Iron industry;
Steel Industry;
Fuel gas operation (FGO) management;
Reheating furnace;
FGO evaluation model;
Fuel gas per ton steel (FGTS) time-series;
Working groups;
Working shifts

**Corresponding author:*
road_lu12@163.com
(Lu, B.)

Article history:
Received 26 March 2020
Revised 9 July 2020
Accepted 13 July 2020

1. Introduction

The iron and steel industry, whose products are widely used in various industries, is the pillar of the manufacturing industry [1]. Therefore, the development of iron and steel industry (whether technological innovation or economic operation) has attracted much attention of many scholars from different countries, such as the United States of America [2], China [3-4], Great Britain [5] etc. With the rapid development of iron and steel industry, the energy consumption is also increasing [6-7] (especially in China, as shown in Fig. 1 [8], million ton coal equivalent (Mtce)). And the energy consumption in iron and steel industry accounts for about 23.6 % of the whole industrial energy consumption in China 2012 [9]. Accordingly, many energy conservation technologies and methods are widely used in iron and steel industry, such as waste energy recovery [10], material flow balance analysis [11] etc. Then, the energy efficiency of iron and steel industry has been greatly improved. However, energy conservation of iron and steel industry should still be further developed [12]. It has been demonstrated that there is considerable potential for energy conservation and emissions reduction in iron and steel industry [13-14].

Reheating furnace, which is widely applied to rolling process [15], is a very important thermal equipment. The energy consumption of reheating furnace accounts for approximately 15-20 % of the total energy consumption in steel industries and approximately 70 % of the rolling process [16]. Therefore, the energy saving of reheating furnace has been an area of intense investigation.

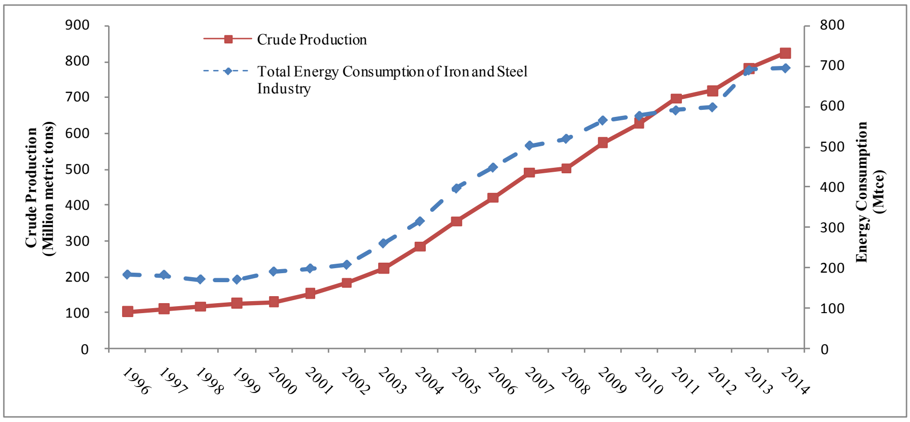

Fig.1 The crude production and energy consumption of Chinese iron and steel industry over the years (Data Source: CHINA STATISTICAL YEARBOOK)

2. Literature review

The research on energy conservation of reheating furnace has been highly valued all the time. Generally, the research work is mainly carried out as follows: thermal regulation optimization, combustion process optimization, waste heat recovery and utilization.

1) Thermal regulation optimization

Energy waste will be effectively reduced, if a reasonable thermal regulation is adopted. Furthermore, thermal regulation optimization can be achieved through billet heat transfer process analysis. The study on billet heat transfer process mainly focus on variation rule of billet heat transfer characteristics under various production rhythm(s) and different loading temperature(s). The reasonable gas supply strategy, which can improve billet heat quality and energy saving, should be formulated in accordance with these variation rules. The numerical analysis method is wildly applied to this field. Mayr *et al.* [17] put forward a time saving simulation of an 18 MW pusher type reheating furnace with a production capacity of 60 t/h and it is fired by natural gas burners. Tang *et al.* [18] developed a transient three-dimensional Computational Fluid Dynamics (CFD) model, which could simulate the flow characteristics, combustion process and multi-scale heat transfer inside the reheating furnace. The validation on an industrial walking beam slab reheating furnace was conducted. Han *et al.* used the finite-volume method to simulate the slab heating characteristics [19]. Although these CFD analyses can be used for accurate prediction of the thermal and combusting fluid characteristics in reheating furnace, it necessitates long computational time and resulting costs due to many governing equations, complexity of the furnace structure and uncertainty of the models [20].

2) Combustion process optimization

Combustion process optimization can improve the fuel gas combustion efficiency through the improvement of burner, the optimization of fuel gas-supply, air-fuel ratio control or other technical means. For example, García and Amel [21] presented a numerical simulation of the effects of using self-recuperative burners, which can utilize heat recovery on the performance of a walking-beam reheating furnace. A transient radiative slab heating analysis was performed to investigate the effect of various fuel mixtures on the performance of an axial-fired reheating furnace

[22]. Meanwhile, the approach, which applied oxy-fuel combustion instead of air-fuel combustion, could enhance combustion efficiency [23]. Moreover, Jian-Guo Wang [24] put forwards a soft-sensing method, which can predict combustion efficiency, since it cannot be measured directly.

3) Waste heat recovery and utilization

Waste heat of flue gas and vaporization cooling system accounts for about 50 % of the energy consumption in reheating furnace [25]. Moreover, the temperature of the flue gas leaving the furnace hearth is about 850 °C [26]. Therefore, the waste heat of flue gas has recovery value. The Organic Ranking Cycle, which has been successfully applied to reheating furnace, is a very effective technology in waste heat recovery [27-28]. Moreover, energy cascade utilization technology has also been applied to recovery of reheating furnace [29].

The above researches mainly concentrated on how to achieve energy saving of reheating furnace through the improvement of technical measures. These technical measures mainly seek new breakthroughs from objective factor. Unfortunately, the influence of subjective factors, which are significant for energy saving of reheating furnace, has not been taken into account. For example, there are differences in the FGO for various WGs in different WSs due to individual operation skills, fatigue state etc. Moreover, Lu *et al*. [30] had proposed an energy apportionment model, which could calculate the energy consumption amount for every billet, in reheating furnace. Then, bottleneck of slab thermal efficiency had been further analyzed [31] and variation of fuel gas consumption had been discussed based on energy consumption model [32] in reheating furnace. However, the FGO for various WGs in different WSs could not be evaluated. This paper proposes a novelty time-series FGO evaluation method, which can evaluate the FGO of various WGs in different WSs.

3. Methodology

3.1 The FGTS in $[T_l, T_{l+1}]$ time interval

Take $[T_l, T_{l+1}]$ time interval as an example, the calculation process of the FGTS is described in detail. Suppose there are f accumulative time segments (ATSs, as shown in reference [30, 32] for the ATS definition) in $[T_l, T_{l+1}]$ time interval (as shown in Fig. 2.), three possible scenarios are as follows:

- G_1 (Starting time: (T_l); Ending time (t_1): the first change moment of billet number (loading time or unloading time) in $[T_l, T_{l+1}]$ time interval);
- G_f (Starting time (t_{f-1}): the last change moment of billet number in $[T_l, T_{l+1}]$ time interval; Ending time: T_{l+1});
- G_i (Starting time (t_{i-1}): the $(i-1)^{\text{th}}$ change moment of billet number; Ending time (t_i): the i^{th} change moment of billet number, $i = 2, 3 \cdots f-1$).

3.1.1 The fuel gas-supply amount in the i^{th} ATS

Correspondingly, the calculation processes of fuel gas-supply for three scenarios are as follows:

- $i = 1$

$$G_1 = \frac{t_{1,1} - T_l}{T_s} \cdot E_{1,1} \cdot T_s + \sum_{j=1}^{n_1} E_{1,j} \cdot T_s + \frac{t_1 - t_{1,n_1}}{T_s} \cdot E_{2,1} \cdot T_s \tag{1}$$

G_1 is the fuel gas-supply amount in the first ATS in GJ. The other variables are shown in Fig. 2.

- $i = f$

$$G_f = \frac{t_{f,1} - t_{f-1}}{T_s} \cdot E_{f,1} \cdot T_s + \sum_{j=1}^{n_f} E_{f,j} \cdot T_s + \frac{T_{l+1} - t_{f,x}}{T_s} \cdot E_{f,x} \cdot T_s \tag{2}$$

G_f is the fuel gas-supply amount in the f^{th} ATS in GJ. The other variables are shown in Fig. 2.

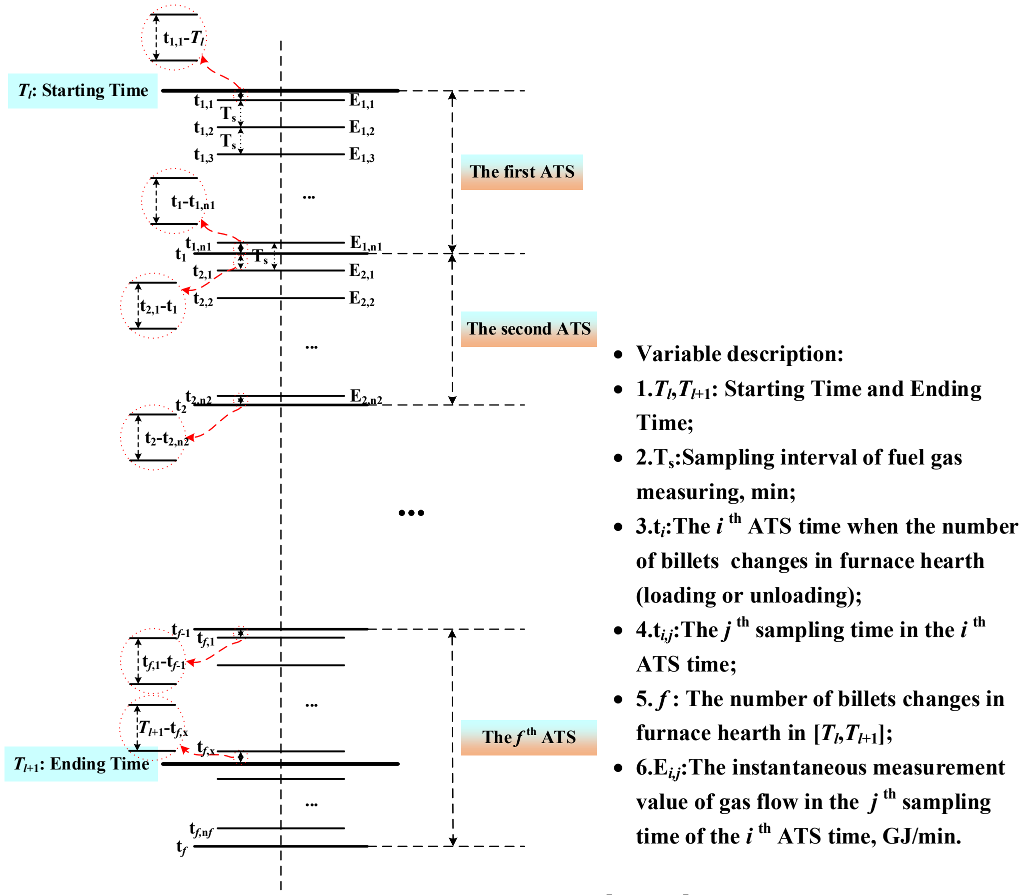

Fig. 2 The calculation process of the FGTS in $[T_l, T_{l+1}]$ time interval

- $i \neq 1 \,\&\, i \neq f$

$$G_i = \frac{t_{i,1} - t_{i-1}}{T_s} \cdot E_{i,1} \cdot T_s + \sum_{j=1}^{n_i} E_{i,j} \cdot T_s + \frac{t_i - t_{i,n_i}}{T_s} \cdot E_{i+1,1} \cdot T_s \tag{3}$$

G_i is the fuel gas-supply amount in the i^{th} ATS in GJ. The other variables are shown in Fig. 2.

3.1.2 The billets weight of furnace hearth in the i^{th} ATS (including $i = 1$ and $i = f$)

According to ATS definition, there is no loading billet or unloading billet in ATS. Therefore, the billets weight of furnace hearth in the i^{th} ATS can be denoted as:

$$M_i = \sum_{k=1}^{N_i} m_{i,k} \tag{4}$$

M_i is the billets weight of furnace hearth in the i^{th} ATS in tons, $m_{i,k}$ is the k^{th} billet weight of furnace hearth in the i^{th} ATS in tons, and N_i is the billet number of furnace hearth in the i^{th} ATS.

3.1.3 The FGTS value in the i^{th} ATS

The FGTS value can be calculated in the i^{th} ATS:

$$e_i = \frac{G_i}{M_i} \tag{5}$$

e_i is the FGTS value in the i^{th} ATS, $i = 1 \cdots f$ in GJ/tons.

3.1.4 The FGTS value in $[T_l, T_{l+1}]$ time interval

The FGTS value can be calculated in $[T_l, T_{l+1}]$ time interval:

$$e_{[T_l,T_{l+1}]} = \frac{\sum_{i=1}^{f} e_i}{f} \tag{6}$$

$e_{[T_l,T_{l+1}]}$ is the FGTS value in $[T_l, T_{l+1}]$ time interval in GJ/tons.

3.2 The FGTS time-series data set in statistical period

The FGTS value can be calculated in $[T_l, T_{l+1}]$ time interval through calculation method in Section 3.1. Then, the statistical period can be divided into several equal time intervals (time intervals: $\Delta T = T_{l+1} - T_l$). Afterwards, the FGTS time-series can be achieved.

Moreover, the FGTS time-series data set can be denoted in statistical period, as shown in Eq. 7.

$$R = \left\{ e_{[T_l,T_{l+1}]} \middle| l \in Integer\ and\ 1 \leq l \leq r-1 \right\} \tag{7}$$

R is the FGTS time-series data set, and r is the amount of time-intervals in statistical period.

3.3 The FGTS time-series data set division according to working schedule

Reheating furnace implements 24-hour continuous working schedule. Moreover, this working schedule consists mainly of two important components (WGs and WSs). Therefore, the FGTS time-series data set can be disaggregated by various WGs and WSs. In general, working schedule mainly includes 'Four Shifts Three Operation Production Mode' and 'Three Shifts Two Operation Production Mode'.

'Four Shifts Three Operation Production Mode': 24 hours in one day are divided into day working shift (DWS, from 0 o'clock to 8 o'clock), swing working shift (SWS, from 8 o'clock to 16 o'clock), night working shift (NWS, from 16 o'clock to 24 o'clock). There are four WGs in turn.

'Three Shifts Two Operation Production Mode': 24 hours in one day are divided into DWS (from 8 o'clock to 20 o'clock), NWS (from 20 o'clock to 8 o'clock next day). There are three WGs in turn.

Therefore, the FGTS time-series data set can be divided according to working schedule. Then, the FGTS time-series data sets of various WGs and WSs can be denoted as data set according to the working schedule, as shown in Eq. 8.

$$P_{u,v} = \left\{ e_{[T_l,T_{l+1}]} \middle| l \in Integer\ \&\ 1 \leq l \leq r-1\ \&\ [T_l, T_{l+1}] \in the\ u^{th}\ WG\ \&\ [T_l, T_{l+1}] \in the\ v^{th}\ WS \right\} \tag{8}$$

$P_{u,v}$ is the FGTS time-series data set of the u^{th} WG in the v^{th} WS, $u = 1 \cdots U$, $v = 1 \cdots V$, $P_{u,v} \in R$.

3.4 The establishment of the FGO evaluation model

These elements in FGTS time-series data sets are continuous data, which is suitable for boxplot analysis [33-34]. The boxplot can qualitatively describe the distribution differences between various data sets. Unfortunately, the quantitative description of these differences is indistinct. Therefore, on the premise of the production process of reheating furnace, the FGO evaluation model, which can quantitatively assess distribution of various data sets, can be established in this paper.

The boxplot parameters of $P_{u,v}$ data set can be recorded as $Q_{2(u,v)}$, $IQR_{(u,v)}$, $UW_{(u,v)}$, $LW_{(u,v)}$. Then, it is should be noted as follows before the FGO evaluation model establishment.

- $Q_{2(u,v)}$, which represents the overall fuel gas consumption level of various data sets, is the benchmark.
- $IQR_{(u,v)}$, which represents data concentration in the 25-75 % range, is the major composition.
- $UW_{(u,v)}$, which represents data concentration in the 75-100 % range, is the supplement.
- $LW_{(u,v)}$, which represents data concentration in the 0-25 % range, is also the supplement.

<u>*Data normalization*</u>

Data normalization, which can eliminate the influence of magnitude order and dimension, is an effective method. Then, Min-Max Normalization is adopted in this paper. Take Q_2 ($Q_2 =$

$\{Q_{2(1,1)}, \cdots Q_{2(1,V)}, Q_{2(2,1)}, \cdots Q_{2(2,V)}, \cdots Q_{2(U,V)}\}$) data set as an example, data normalization is described in detail, as shown in Eq. 9.

$$Q'_{2(u,v)} = \frac{Q_{2(u,v)} - min(Q_2)}{max(Q_2) - min(Q_2)} \tag{9}$$

$Q'_{2(u,v)}$ is the 50th percentile of the u^{th} WG in the v^{th} WS after normalization, $Q_{2(u,v)}$ is the 50th percentile of the u^{th} WG in the v^{th} WS before normalization. $\min(Q_2)$ and $\max(Q_2)$ are the minimum value and maximum value in Q_2 data set, respectively. $IQR'_{(u,v)}$ is the interquartile rage of the u^{th} WG in the v^{th} WS after normalization, $UW'_{(u,v)}$ is the upper whisker of the u^{th} WG in the v^{th} WS after normalization, and $LW'_{(u,v)}$ is the lower whisker of the u^{th} WG in the v^{th} WS after normalization.

Modelling

Then, the FGO evaluation model of the u^{th} WG in the v^{th} WS can be defined as follow:

$$ID_{(u,v)} = \alpha_1 \cdot Q'_{2(u,v)} + \alpha_2 \cdot IQR'_{(u,v)} + \alpha_3 \cdot UW'_{(u,v)} + \alpha_4 \cdot LW'_{(u,v)} \tag{10}$$

$ID_{(u,v)}$ is the FGO evaluation value of the u^{th} WG in the v^{th} WS, [0,1]. $\alpha_1, \alpha_2, \alpha_3, \alpha_4$ are the weighting coefficients of $Q'_{2(u,v)}, IQR'_{(u,v)}, UW'_{(u,v)}, LW'_{(u,v)}$, respectively.

According to the weighting description hypotheses, the importance of four variables is shown in descending order.

$$Q'_{2(u,v)} > IQR'_{(u,v)} > UW'_{(u,v)} = LW'_{(u,v)}$$

Therefore, $\alpha_1 > \alpha_2 > \alpha_3 = \alpha_4$ in turn in this FGO evaluation model.

It is worth noting that the FGO evaluation model, which is put forward in this manuscript, is to evaluate the FGO of various WGs and WSs. In order to ensure of the evaluation effectiveness, it is necessary to select the production data of normal production.

4. Case study – Results and discussion

The No. 1 reheating furnace of a rolling mill is considered as research object. The main product of this reheating furnace is medium-plate (length: 8000-10000mm; width: 1200-2000mm; thick: 220-230mm). The production data are analyzed as the basic data sources in June and July 2016. In this period, the production process of No. 1 reheating furnace is relatively stable, which is convenient for FGO evaluation analysis.

4.1 The working schedule of No. 1 reheating furnace

'Four Shifts Three Operation Production Mode' has been adopted in this No. 1 reheating furnace. The working schedule, which derives from the production record, for this reheating furnace in June and July 2016 has also been shown in Table 1.

Table 1 The working schedule of No.1 reheating furnace in June and July 2016

A WG	NWS	NWS	OD	DWS	DWS	SWS	SWS	OD
B WG	OD	DWS	DWS	SWS	SWS	OD	NWS	NWS
C WG	DWS	SWS	SWS	OD	NWS	NWS	OD	DWS
D WG	SWS	OD	NWS	NWS	OD	DWS	DWS	SWS
June								1
	2	3	4	5	6	7	8	9
	10	11	12	13	14	15	16	17
	18	19	20	21	22	23	24	25
	26	27	28	29	30			
July						1	2	3
	4	5	6	7	8	9	10	11
	12	13	14	15	16	17	18	19
	20	21	22	23	24	25	26	27
	28	29	30	31				

Noted: Off-Duty (OD)

As shown in Table 1, the working status of various WGs is presented clearly in different WSs. Due to 24-hour continuous working mode of reheating furnace, the $[T_l, T_{l+1}]$ time interval can be defined as 1 hour for convenient calculation. Furthermore, the FGTS per an hour (FGTSH) can be defined.

4.2 The calculation and discussion of FGTSH

There are 1464 FGTSHs can be achieved through calculation in statistical period. Then, these FGTSHs can be classified according to Section 3.3 (as shown in Table 2). The FGTSH boxplot of various WGs in different WSs is shown in Fig. 3.

It should be noted that the outliers are not under consideration due to their small proportion. The results after normalization and the FGO evaluation value of each WG in various WSs can be calculated through Eqs. 9 and 10 (as shown in Table 3, $\alpha_1 = 0.4$, $\alpha_2 = 0.3$, $\alpha_3 = 0.15$, $\alpha_4 = 0.15$).

Table 2 The FGTSHs division for various WGs and WSs

The number of FGTSH	A WG	B WG	C WG	D WG	Total
The DWS	122	132	111	118	483
The SWS	126	121	119	120	486
The NWS	139	122	108	126	495
Total	387	375	338	364	1464

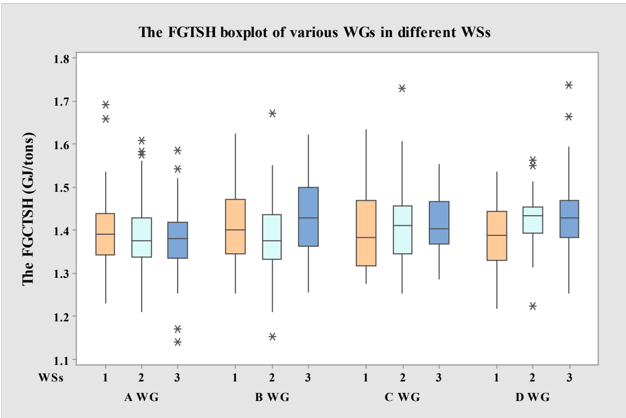

Fig. 3 The FGTSH boxplot of various WGs in different WSs
Noted: 1: DWS; 2: SWS; 3: N WS.

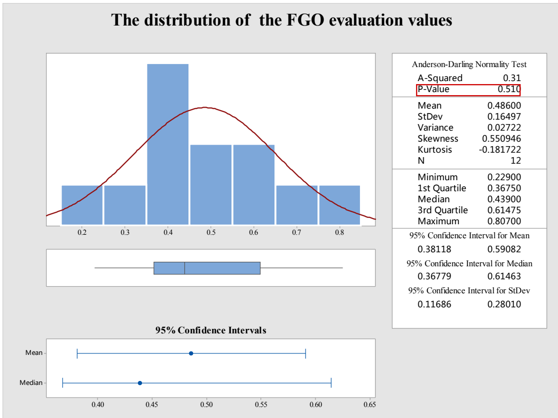

Fig. 4 The FGO evaluation values distribution

Table 3 The value of $Q'_{2(u,v)}$, $IQR'_{(u,v)}$, $UW'_{(u,v)}$, $LW'_{(u,v)}$ and the FGO evaluation value for WGs in various WSs

Type	A WG			B WG			C WG			D WG		
(Normalization)	DWS	SWS	NWS	DWS	SWS	NWS	DWS	SWS	NWS	DWS	SWS	NWS
$Q'_{2(u,v)}$	0.241	0	0.086	0.448	0.017	0.897	0.103	0.603	0.483	0.207	1	0.931
$IQR'_{(u,v)}$	0.097	0.092	0.082	0.697	0.461	0.82	1	0.539	0.382	0.551	0	0.258
$UW'_{(u,v)}$	0.349	0.689	0.415	0.896	0.519	0.594	1	0.858	0.274	0.302	0	0.623
$LW'_{(u,v)}$	0.802	0.965	0.453	0.57	0.93	0.756	0	0.57	0.465	0.826	0.395	1
The FGO evaluation value	0.384	0.346	0.229	0.608	0.362	0.807	0.491	0.617	0.419	0.417	0.459	0.693

4.2.1 The FGO evaluation model validation

The FGO evaluation values of various WGs in different WSs are accorded with normal distribution due to P-Value (0.51) > 0.05 (as shown in Fig. 4, this data analysis has been done in Minitab 17.0). That is, the FGO evaluation values mainly concentrate on [0.2, 0.8] range (account for 91.7 % of total number), especially for [0.2, 0.6] range (account for 66.67 % of total number). Therefore, the FGO evaluation model is reasonable. It is worth mentioning that there are no FGO evaluation values less than 0.2. Thus, there is still room for improvement in the FGO of various WGs in different WSs. Additionally, the FGO evaluation values, which are higher than 0.8, should be emphasized due to the higher fuel gas consumption, such as the NWS of B WG.

4.2.2 The FGO evaluation results analysis

The following analysis results can be achieved.

- The FGO evaluation values analysis of each WG in various WSs

A WG: The FGO of A WG in all WSs is very well due to its lower FGO evaluation values. Nevertheless, there is still room for improvement in the FGO for A WG. Because the Q_2 value is lower than others, the FGO evaluation value is relatively small. Unfortunately, the IQR and whisker are not optimal. Therefore, the enhancement of fuel gas consumption centralization is an effective method to improve the FGO of A WG.

B WG: the FGO of B WG varies greatly in three WSs. Comparing with A WG, the performance of SWS, which is better than the other WSs, still has a certain gap. Because of the high value of Q_2, IQR and whisker in DWS and NWS, the FGO evaluation value has deteriorated further. Therefore, the DWS and NWS should be given more attention, especially for NWS.

C WG and D WG: the FGO evaluation value is mainly distributed in [0.4, 0.7] for C WG and D WG in three WSs. This distribution is determined by the following three conditions: i) The higher Q_2 value, the lower IQR and whisker value, such as the SWS of D WG; ii) The lower Q_2 value, the higher IQR and whisker value, such as DWS of C WG and DWS of D WG; iii) The medium of Q_2, IQR value and whisker value, such as the other WSs of C WG and D WG. Therefore, appropriate energy saving measures should be adopted according to different conditions.

- The FGO evaluation values analysis of each WS in various WGs

DWS: The FGO evaluation values of various WGs are 0.384 (A WG), 0.608 (B WG), 0.491 (C WG), 0.417 (D WG), respectively. The performance of A WG is optimal due to the lower Q_2, IQR and whisker. The Q_2 value of D WG is slightly lower than that of A WG, yet the IQR of D WG is larger than that of A WG. Therefore, the FGO of D WG is still lower than that of A WG. There is not much difference between C WG and D WG. Because the Q_2 value of B WG is more larger than that of others, the performance of B WG is the worst.

SWS: The FGO evaluation values of different WGs are 0.346 (A WG), 0.362 (B WG), 0.617 (C WG), 0.459 (D WG), respectively. The FGO of A WG and B WG performs better than the other WGs. Although the IQR value of D WG is lower than other WGs, the Q_2 value of D WG is much larger than that of the other WGs. Therefore, the performance of D WG is either mediocre. Then, the FGO of C WG is the lowest due to the higher Q_2 value and IQR value.

NWS: The FGO evaluation values of different WGs are 0.229 (A WG), 0.807 (B WG), 0.419 (C WG), 0.693 (D WG), respectively. Obviously, the performance of A WG is much higher than that of other WGs, followed by C WG and D WG due to the medium Q_2 value and IQR value. It is worth mentioning that the FGO of B WG is worst because its Q_2 value and IQR value are much higher than that of the other WGs.

4.3 Main findings

4.3.1 The primary reasons of FGO evaluation values' difference

Actually, the FGO of various WGs in different WSs can be evaluated through two indicators, that is, the average value and the standard deviation value of individual FGTSH data set. On one hand, the average values of various FGTSH data sets indicate fuel gas consumption level of various WGs in different WSs. On the other hand, the standard deviation values of various FGTSH data sets represent gas consumption fluctuation of various WGs in different WSs. Unfortunately, it is inconvenient for these two indicators to evaluate the FGO due to dimensional difference and their uncertain influence degree on the FGO. Therefore, the FGO evaluation model based on box-plot is proposed in this paper. The ranking results of the FGO evaluation values are as follows in ascending order (as shown in Table 3): NWS(A WG:0.229), SWS(A WG:0.346), SWS(B WG:0.362), DWS(A WG:0.384), DWS(D WG:0.417), NWS(C WG:0.419), SWS(D WG:0.459), DWS(C WG:0.491), DWS(B WG:0.608), SWS(C WG:0.617), NWS(D WG:0.693), NWS(B WG:0.807). Then, the ranking results of the FGO evaluation values, the average values and the standard deviation values of individual FGTSH data sets are all shown in Fig. 5.

There are three possible scenarios between the FGO evaluation values and two indicators (as shown in Fig. 5).

- The FGO evaluation value is relatively lower because of the smaller the average value and the standard deviation value of FGTSH data sets, such as NWS (A WG);
- The FGO evaluation value is relatively higher because of the larger the average value and the standard deviation value of FGTSH data sets, such as NWS (B WG);
- The FGO evaluation value is undetermined due to the uncertainty of the average value and the standard deviation value of FGTSH data sets. For example, although the average value of SWS (B WG) FGTSH data set is higher than that of DWS (A WG) FGTSH data set, the FGO evaluation value of SWS (B WG) is superior to that of DWS (A WG) because of the lower the standard deviation value of SWS (B WG) FGTSH data set. Similarly, this phenomenon also happens between SWS (D WG) and DWS (C WG) etc.

The FGO evaluation values can reflect these two indicators synthetically. Then, the FGO evaluation values can represent the FGO of various WGs in different WSs. Meanwhile, the validation of the FGO evaluation model has also been further verified.

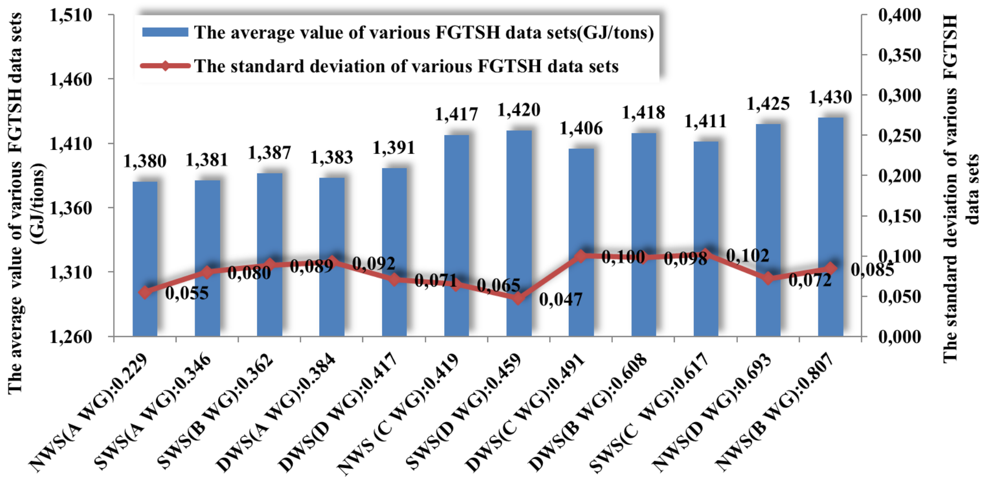

Fig. 5 The FGO evaluation values, the average value and the standard deviation of individual FGTSH data set

4.3.2 The establishment of the reward and punishment system

For improving employees' awareness of energy conservation, the reward and punishment system should be established.

Firstly, the FGO evaluation grade should be formulated. For example, the FGO evaluation grade can be divided into five levels according to FGO evaluation value. That is, [0, 0.2): Excellent grade; [0.2, 0.4): Good grade; [0.4, 0.6): Mean grade; [0.6, 0.8): Poor grade; [0.8, 1]: Failed grade (as shown in Fig. 6).

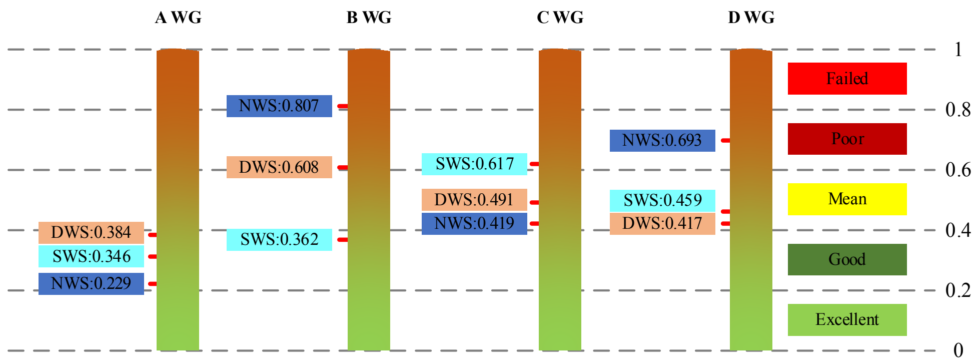

Fig. 6 The FGO evaluation grade of various WGs in different WSs

As shown in Fig. 6, there are four FGTSH data sets in Good grade, DWS (A WG), SWS (A WG), NWS (A WG), SWS (B WG), respectively; four FGTSH data sets in Mean grade, DWS (C WG), NWS (C WG), DWS (D WG) and SWS (D WG), respectively; three FGTSH data sets in Poor grade, DWS (B WG), SWS (C WG), NWS (D WG), respectively; one FGTSH data set in Failed grade, NWS (B WG). Moreover, two points should be concerned about:

- The FGO evaluation grade difference of B WG is obvious in various WSs, DWS (B WG): Poor grade; SWS (B WG): Good grade; NWS (B WG): Failed grade. Therefore, the B WG should be focused on.
- There is no FGCSH data set can reach Excellent grade. Thus, this reheating furnace has great energy saving potential in terms of operation.

Secondly, the reward and punishment system should be established in accordance to FGO evaluation grade.

1) The determination of FGO evaluation period

Generally, wage settlement cycle can be regarded as FGO evaluation period for payment convenience, such as one month (especially for Chinese enterprises).

2) The establishment of reward and punishment rules

i) Evaluation benchmark
Mean grade can be used as evaluation benchmark. That is, neither reward nor punishment will be given when the FGO evaluation grade is Mean grade.

ii) The principle of cascade reward and punishment
The principle of cascade reward and punishment mainly entails a certain proportion of rewards should be given when FGO evaluation grade is higher one level than Mean grade, such as Good grade: 20 % rewards. A higher proportion of rewards should be given when FGO evaluation grade is higher one level than before, such as Excellent grade: 50 % rewards, and vice versa. In order to pursue more profits, employees actively enhance their skills and improve their FGO. Then, the operation energy saving of reheating furnace can be achieved.

4.3.3 The FGO improvement measures

Essentially, the FGO evaluation grades of various FGTSH data sets are determined by their respective FGO evaluation values. Therefore, the FGO evaluation values should be further improved. Generally, there are three ways to improve the FGO evaluation values according to the analysis results of Section 4.2.

- Q_2 value

The lower Q_2 value is the major way to improve FGO evaluation value because of the dominant function in FGO evaluation model. Q_2 values, which are the median in various FGTSH data sets, represent overall FGO. Moreover, working skills, which is the main way to reduce Q_2 values, should be strengthened for every employee.

- IQR value

IQR value represents the concentration of 25-75 % elements in every FGTSH data set. That is, the smaller the IQR value, the higher 25-75 % elements centralization degree, the higher the FGO, and vice versa. Besides working skills, working responsibility, which determines whether employees are willing to do their jobs better, is also very important. If yes, IQR value will be improved, and vice versa.

- Whisker value

The lower whisker value and the upper whisker value represent the concentration of 0-25 % elements and 75-100 % elements in every FGTSH data set, respectively. The smaller the whisker value, the higher the FGO, and vice versa. However, the lower whisker value and upper whisker value only represent 25 % elements in every FGTSH data set, respectively. Their influence on the FGO evaluation value is relatively limited. Furthermore, working passion determines whether employees want to improve their work better or not. If yes, whisker value will be improved, and vice versa. Therefore, 3W (Working passion, Working responsibility, Working skills) determines the FGO evaluation grade of each FGTSH data set together. That is, the energy saving of reheating furnace in the respect of operation can be achieved through the 3W improvement. How to improve 3W should be paid more attention. Generally, the skills training and the reward and punishment system are the important improvement measures on 3W. The relationship of the improvement measures, the influence object, the influence result is shown in Fig. 7.

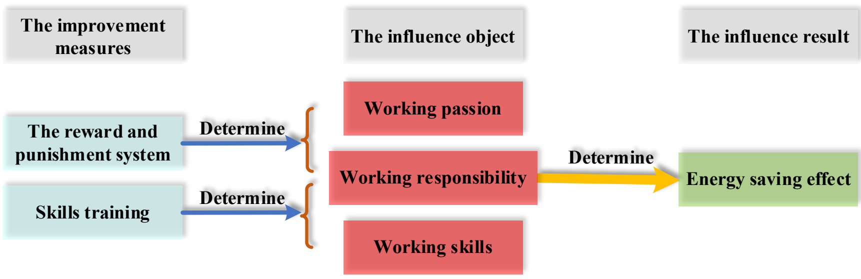

Fig. 7 The relationship between the improvement measures, the influence object and the influence result

5. Conclusion

A new time-series FGO evaluation model, which can evaluate the FGO of various WGs in different WSs, has been established in this paper. This time-series FGO evaluation model mainly includes: i) The FGTS in $[T_l, T_{l+1}]$ time interval; ii) The FGTS time-series data set in statistical period; iii) The FGTS time-series data set division according to working schedule; iv) The establishment of the FGO evaluation model. Then, this FGO evaluation model has been successfully applied to the FGO evaluation for various WGs in different WSs in a reheating furnace.

The main conclusions are as follows:

1) A novelty time-series FGO evaluation model has been put forward in this paper. This model can resolve the problem that FGO of various WGs in different WSs can't be effectively evaluated.
2) Case study shows that the ranking results of the FGO evaluation values are as follows in ascending order in statistical period: NWS (A WG:0.229), SWS (A WG:0.346), SWS (B WG:0.362), DWS (A WG:0.384), DWS (D WG:0.417), NWS (C WG:0.419), SWS (D WG:0.459), DWS (C WG:0.491), DWS (B WG:0.608), SWS (C WG:0.617), NWS (D WG:0.693), NWS (B WG:0.807). The evaluation result shows that:
   - For various WGs, the A WG performs best, followed by C WG and D WG. And the performance of B WG is the worst due to its violent fluctuation of FGO evaluation values in three WSs;
   - For different WSs, the DWS and SWS performs well. Unfortunately, the performance of NWS is unsatisfactory.
3) The discussion results show that:
   - The reward and punishment system should be established according to FGO evaluation grade results;
   - 3W can be enhanced through skills training and the reward and punishment system. The energy saving effect in terms of operation for reheating furnace can be achieved.

Acknowledgement

This research was funded by by National Natural Science Foundation of China (Grant NO. 51804002) and "The APC was funded by 51804002".

Reference

[1] Duan, W., Yu, Q., Wang, K., Qin, Q., Hou, L., Yao, X., Wu, T. (2015). ASPEN plus simulation of coal integrated gasification combined blast furnace slag waste heat recovery system, *Energy Conversion and Management*, Vol. 100, 30-36, doi: 10.1016/j.enconman.2015.04.066.

[2] Karali, N., Park, W.Y., McNeil, M. (2017). Modeling technological change and its impact on energy savings in the U.S. iron and steel sector, *Applied Energy*, Vol. 202, 447-458, doi: 10.1016/j.apenergy.2017.05.173.

[3] Chen, Q., Gu, Y., Tang, Z., Wei, W., Sun, Y. (2018). Assessment of low-carbon iron and steel production with CO_2 recycling and utilization technologies: A case study in China, *Applied Energy*, Vol. 220, 192-207, doi: 10.1016/j.apenergy.2018.03.043.

[4] Lu, B., Tang, K., Chen, D., Han, Y., Wang, S., He, X., Chen, G. (2019). A novel approach for lean energy operation based on energy apportionment model in reheating furnace, *Energy*, Vol. 182, 1239-1249, doi: 10.1016/j.energy.2019.06.076.

[5] Griffin, P.W., Hammond, G.P. (2019). Industrial energy use and carbon emissions reduction in the iron and steel sector: A UK perspective, *Applied Energy*, Vol. 249, 109-125, doi: 10.1016/j.apenergy.2019.04.148.

[6] Lu, B., Chen, G., Chen, D., Yu, W. (2016). An energy intensity optimization model for production system in iron and steel industry, *Applied Thermal Engineering*, Vol. 100, 285-295, doi: 10.1016/j.applthermaleng.2016.01.064.

[7] An, R., Yu, B., Li, R., Wei, Y.-W. (2018). Potential of energy saving and CO_2 emission reduction in China's iron and steel industry, *Applied Energy*, Vol. 226, 862-880, doi: 10.1016/j.apenergy.2018.06.044.

[8] Chen, D., Lu, B., Zhang, X., Dai, F., Chen, G., Liu, Y. (2018). Fluctuation characteristic of billet region gas consumption in reheating furnace based on energy apportionment model, *Applied Thermal Engineering*, Vol. 136, 152-160, doi: 10.1016/j.applthermaleng.2018.03.007.

[9] Chen, D., Lu, B., Chen, G., Yu, W. (2017). Influence of the production fluctuation on the process energy intensity in iron and steel industry, *Advances in Production Engineering & Management*, Vol. 12, No. 1, 75-87, doi: 10.14743/apem2017.1.241.

[10] Zhang, Q., Zhao, X., Lu, H., Ni, T., Li, Y. (2017). Waste energy recovery and energy efficiency improvement in China's iron and steel industry, *Applied Energy*, Vol. 191, 502-520, doi: 10.1016/j.apenergy.2017.01.072.

[11] Zhang, Q., Xu, J., Wang, Y., Hasanbeigi, A., Zhang, W., Lu, H., Arens, M. (2018). Comprehensive assessment of energy conservation and CO_2 emissions mitigation in China's iron and steel industry based on dynamic material flows, *Applied Energy*, Vol. 209, 251-265, doi: 10.1016/j.apenergy.2017.10.084.

[12] He, K., Wang, L. (2017). A review of energy use and energy-efficient technologies for the iron and steel industry, *Renewable and Sustainable Energy Reviews*, Vol. 70, 1022-1039, doi: 10.1016/j.rser.2016.12.007.

[13] Peng, J., Xie, R., Lai, M. (2018). Energy-related CO_2 emissions in the China's iron and steel industry: A global supply chain analysis, *Resources, Conservation and Recycling*, Vol. 129, 392-401, doi: 10.1016/j.resconrec.2016.09.019.

[14] Hu, R., Zhang, Q. (2015). Study of a low-carbon production strategy in the metallurgical industry in China, *Energy*, Vol. 90, Part 2, 1456-1467, doi: 10.1016/j.energy.2015.06.099.

[15] McBrien, M., Cabrera Serrenho, A., Allwood, J.M. (2016). Potential for energy savings by heat recovery in an integrated steel supply chain, *Applied Thermal Engineering*, Vol. 103, 592-606, doi: 10.1016/j.applthermaleng.2016.04.099.

[16] Ke, H.-L., Dong, B., Ye, B. (2014). Research and application of slab heating curve in reheating furnace, *Metallurgical Industry Automation*, Vol. 38, No. 3, 50-55, doi: 10.3969/j.issn.1000-7059.2014.03.010.

[17] Mayr, B., Prieler, R., Demuth, M., Moderer, L., Hochenauer, C. (2017). CFD analysis of a pusher type reheating furnace and the billet heating characteristic, *Applied Thermal Engineering*, Vol. 115, 986-994, doi: 10.1016/j.applthermaleng.2017.01.028.

[18] Tang, G., Wu, B., Bai, D., Wang, Y., Bodnar, R., Zhou, C. (2018). CFD modeling and validation of a dynamic slab heating process in an industrial walking beam reheating furnace, *Applied Thermal Engineering*, Vol. 132, 779-789, doi: 10.1016/j.applthermaleng.2018.01.017.

[19] Han, S.H., Chang, D., Kim, C.Y. (2010). A numerical analysis of slab heating characteristics in a walking beam type reheating furnace, *International Journal of Heat and Mass Transfer*, Vol. 53, No. 19-20, 3855-3861, doi: 10.1016/j.ijheatmasstransfer.2010.05.002.

[20] Emadi, A., Saboonchi, A., Taheri, M., Hassanpour, S. (2014). Heating characteristics of billet in a walking hearth type reheating furnace, *Applied Thermal Engineering*, Vol. 63, No. 1, 396-405, doi: 10.1016/j.applthermaleng.2013.11.003.

[21] García, A.M., Amell, A.A. (2018). A numerical analysis of the effect of heat recovery burners on the heat transfer and billet heating characteristics in a walking-beam type reheating furnace, *International Journal of Heat and Mass Transfer*, Vol. 127, Part B, 1208-1222, doi: 10.1016/j.ijheatmasstransfer.2018.07.121.

[22] Han, S.H., Chang, D. (2012). Radiative slab heating analysis for various fuel gas compositions in an axial-fired reheating furnace, *International Journal of Heat and Mass Transfer*, Vol. 55, No. 15-16, 4029-4036, doi: 10.1016/j.ijheatmasstransfer.2012.03.041.

[23] Han, S.H., Lee, Y.S., Cho, J.R., Lee, K.H. (2018). Efficiency analysis of air-fuel and oxy-fuel combustion in a reheating furnace, *International Journal of Heat and Mass Transfer*, Vol. 121, 1364-1370, doi: 10.1016/j.ijheatmasstransfer.2017.12.110.

[24] Wang, J.-G., Shen, T., Zhao, J.-H., Ma, S.-W., Wang, X.-F., Yao, Y., Chen, T. (2017). Soft-sensing method for optimizing combustion efficiency of reheating furnaces, *Journal of the Taiwan Institute of Chemical Engineers*, Vol. 73, 112-122, doi: 10.1016/j.jtice.2016.09.037.

[25] Zhang, Q. (2017). Application of reheating furnace waste heat integrated utilization technology, *Energy for Metallurgical Industry*. Vol. 36, No. 1, 45-47, doi: 10.3969/j.issn.1001-1617.2017.01.011.

[26] Dal Magro, F., Jimenez-Arreola, M., Romagnoli, A. (2017). Improving energy recovery efficiency by retrofitting a PCM-based technology to an ORC system operating under thermal power fluctuations, *Applied Energy*, Vol. 208, 972-985, doi: 10.1016/j.apenergy.2017.09.054.

[27] Jiménez-Arreola, M., Wieland, C., Romagnoli, A. (2017). Response time characterization of organic rankine cycle evaporators for dynamic regime analysis with fluctuating load, *Energy Procedia*, Vol. 129, 427-434, doi: 10.1016/j.egypro.2017.09.131.

[28] Pili, R., Romagnoli, A., Spliethoff, H., Wieland, C. (2017). Techno-economic analysis of waste heat recovery with ORC from fluctuating industrial sources, *Energy Procedia*, Vol. 129, 503-510, doi: 10.1016/j.egypro.2017.09.170.

[29] Wang, L. (2016). An example of waste heat recovery of heating furnace based on energy cascade utilization, *Metallurgical Power*, Vol. 1, 30-31, doi: 10.3969/j.issn.1006-6764.2016.01.010.

[30] Lu, B., Chen, D., Chen, G., Yu, W. (2017). An energy apportionment model for a reheating furnace in a hot rolling mill – A case study, *Applied Thermal Engineering*, Vol. 112, 174-183, doi: 10.1016/j.applthermaleng.2016.10.080.

[31] Chen, D., Lu, B., Dai, G.-Q., Chen, G., Zhang, X. (2018). Bottleneck of slab thermal efficiency in reheating furnace based on energy apportionment model, *Energy*, Vol. 150, 1058-1069, doi: 10.1016/j.energy.2018.02.149.

[32] Chen, D., Lu, B., Dai, F.-Q., Chen, G., Yu, W. (2018). Variations on billet gas consumption intensity of reheating furnace in different production states, *Applied Thermal Engineering*, Vol. 129, 1058-1067, doi: 10.1016/j.applthermaleng.2017.10.096.

[33] Ferreira, J.E.V., Pinheiro, M.T.S., dos Santos, W.R.S., da Silva Maia, R. (2016). Graphical representation of chemical periodicity of main elements through boxplot, *Educación Química,* Vol. 27, No. 3, 209-216, doi: 10.1016/j.eq.2016.04.007.

[34] Hubert, M., Vandervieren, E. (2008). An adjusted boxplot for skewed distributions, *Computational Statistics & Data Analysis,* Vol. 52, No. 12, 5186-5201, doi: 10.1016/j.csda.2007.11.008.

Appendix

The following abbreviations are used in the paper:

FGO	Fuel gas operation
FGTS	Fuel gas per ton steel
ATS	Accumulative time segment
FGTSH	FGTS per an hour
Mtce	Million ton coal equivalent
CFD	Computational fluid dynamics
WG	Working group
A WG	A working group
B WG	B working group
C WG	C working group
D WG	D working group
WS	Working shift
DWS	Day working shift
SWS	Swing working shift
NWS	Night working shift
OD	Off-Duty